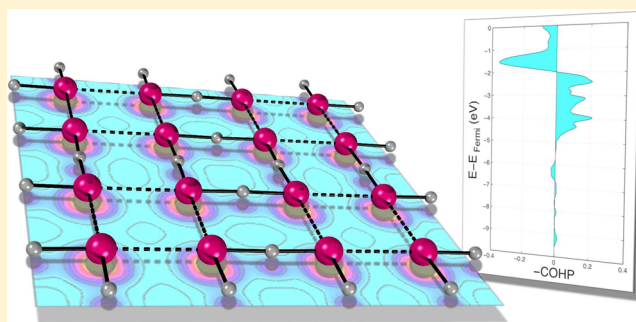


Electronic Structure of Ternary Rhodium Hydrides with Lithium and Magnesium

Jonas Nils Becker,[†] Jessica Bauer,[†] Andreas Giehr,[†] Pui Ieng Chu,[†] Nathalie Kunkel,[†] Michael Springborg,^{*,†,‡} and Holger Kohlmann^{*,§}[†]Physical and Theoretical Chemistry, Saarland University, 66123 Saarbrücken, Germany[‡]School of Materials Science and Engineering, Tianjin University, Tianjin 300072, People's Republic of China[§]Institute of Inorganic Chemistry, Leipzig University, 04103 Leipzig, Germany

ABSTRACT: Chemical bonding in and electronic structure of lithium and magnesium rhodium hydrides are studied theoretically using DFT methods. For Li_3RhH_4 with planar complex RhH_4 structural units, Crystal Orbital Hamilton Populations reveal significant Rh–Rh interactions within infinite one-dimensional ${}^1_\infty[\text{RhH}_4]$ stacks in addition to strong rhodium–hydrogen bonding. These metal–metal interactions are considerably weaker in the hypothetical, heavier homologue Na_3RhH_4 . Both compounds are small-band gap semiconductors. The electronic structures of Li_3RhH_6 and Na_3RhH_6 with rhodium surrounded octahedrally by hydrogen, on the other hand, are compatible with a classical complex hydride model according to the limiting ionic formula $(\text{M}^+)_3[\text{RhH}_6]^{3-}$ without any metal–metal interaction between the 18-electron hydridorhodate complexes. In MgRhH , building blocks of the composition $(\text{RhH}_2)_4$ are formed with strong rhodium–hydrogen and significant rhodium–rhodium bonding (bond lengths of 298 pm within Rh_4 squares). These units are linked together to infinite two-dimensional layers ${}^2_\infty[(\text{RhH}_{2/2})_4]$ via common hydrogen atoms. Li_3RhH_4 and MgRhH are accordingly examples for border cases of chemical bonding where the classical picture of hydridometalate complexes in complex hydrides is not sufficient to properly describe the chemical bonding situation.



I. INTRODUCTION

Hydrogen is a very versatile inorganic ligand with chemical bonding ranging from ionic to metallic and covalent. Ternary and multinary metal hydrides $\text{M}_m\text{M}'_m\text{H}_n$ with M being an alkaline, alkaline earth, or rare earth metal and M' being a late transition metal often belong to the group of complex hydrides, with Na_2PtH_4 ,¹ Mg_2FeH_6 ,² and Eu_2IrH_5 ³ being typical examples. They contain 18- or 16-electron hydridometalate anions such as $[\text{FeH}_6]^{4-}$, $[\text{PtH}_4]^{2-}$, and $[\text{IrH}_5]^{4-}$ in which hydrogen is bonded covalently to the transition metal. These complex anions are counterbalanced by cations of the less electronegative metal M ; that is, the chemical bonding in complex metal hydrides comprises covalent as well as ionic bonding. This simple picture is a good approximation as long as the electron transfer from the cations to the complex hydridometalate anions is more or less complete. For the lighter alkaline and alkaline earth metals with higher electronegativity, however, deviations from this behavior and interesting border cases of chemical bonding may be expected. Complex hydrides of ruthenium and rhodium with lithium or magnesium indeed show unusual geometries of the hydridometalate anions in agreement with a more complicated chemical bonding beyond that described by the 18-electron rule.

The purpose of the present work is to use theoretical methods to obtain a more detailed understanding of the chemical bonding in the latter systems. Some understanding has been obtained from earlier theoretical studies on complex ruthenium hydrides,^{4,5} but here we shall extend those by adding a more detailed analysis and by considering also lithium and magnesium rhodium hydrides that, to the best of our knowledge, have not been treated theoretically earlier.

Within the ternary system $\text{Li}-\text{Rh}-\text{H}$, the existence of two phases has been reported, Li_3RhH_6 ⁶ and Li_3RhH_4 .⁷ Li_3RhH_6 may be regarded as a classical complex hydride with 18-electron hexahydridorhodate(III) complexes $[\text{RhH}_6]^{3-}$. The complex anions are isolated from each other, and the smallest Rh–Rh distance is 480 pm. On the other hand, Li_3RhH_4 contains planar tetrahydridorhodate(I) $[\text{RhH}_4]^{3-}$ units (cf., Figure 1), which might be regarded as 16-electron complexes.⁶ A weak Rh–Rh interaction was proposed on the basis of Rh–Rh distances of 387 pm within the stacks of tetrahydridorhodate(I) units running along the crystallographic a axis (Figure 1).⁶ Notice that we here and below have used crystal structure data based on the deuterides instead of the hydrides whereby the deuterium positions have been determined using neutron

Received: October 25, 2013

Published: December 27, 2013

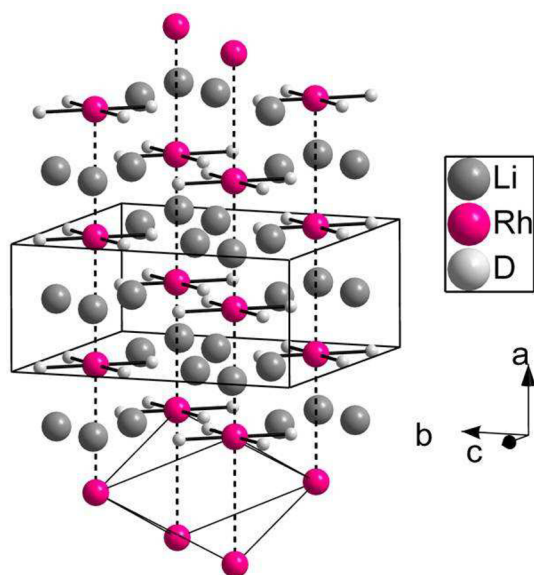


Figure 1. Crystal structure of Li_3RhH_4 from the deuteride data of ref 6. Solid lines represent covalent Rh–H bonding within the $[\text{Rh}_4\text{H}_4]^{3-}$ complexes, whereas the dashed lines indicate the nearest-neighbor Rh–Rh distances (387 pm). Next-nearest neighbor distances of 488 pm are indicated in the lower part of the figure by thin solid lines.

diffraction experiments. However, isotope effects are generally sufficiently small to be unimportant for the conclusions drawn in the present work. More details on isotope effects of hydrogen in hydrogenous compounds, including of $\text{Na}_3\text{Rh}(\text{H}/\text{D})_6$, can be found elsewhere.^{8–10}

For the ternary system Mg–Rh–H, the two phases MgRhH_{1-x} and $\text{Mg}_2\text{RhH}_{1.1}$ have been identified.^{11–13} The latter is a typical intercalation compound in which hydrogen occupies octahedral and tetrahedral voids in a Ti_2Ni -type arrangement of magnesium and rhodium atoms¹³ with the closest Rh–Rh contacts being 317 pm. Such nonstoichiometric intercalation-type hydrides are also frequently encountered in the combination rare earth–rhodium–hydrogen.^{14,15} In MgRhD_{1-x} , no clearly discernible hydridometallate complexes have been found.^{11,12} Its crystal structure is related to the cubic perovskite type and can be regarded as a tetragonally distorted vacancy variant of this.¹⁶ A striking feature of the crystal structure of MgRhH_{1-x} is the tetrameric $[\text{Rh}_4\text{H}_4]$ units (cf., Figure 2). Clustering may be expected for such an electron-poor compound, although little is known about its chemical bonding. A further complication in this case is the lack of stoichiometry with respect to hydrogen. Depending on the synthesis conditions, the hydrogen content varies for MgRhH_{1-x} in the range $0.06(2) \leq x \leq 0.39(1)$.¹¹ For both magnesium rhodium hydrides, MgRhH_{1-x} and $\text{Mg}_2\text{RhH}_{1.1}$, no physical properties beyond crystal structures have been reported so far.

In this work, we shall use theoretical calculations in studying the electronic properties of Li_3RhH_4 and MgRhH_{1-x} with special emphasis on their chemical bonding whereby we shall obtain a more general understanding that can be applied to other, related compounds. To test our approach on systems with a simpler type of chemical bonding, we have also included Li_3RhH_6 as an example of systems that presumably are lacking metal–metal bonding. Furthermore, we extend our studies to the analogous compounds with the higher homologues of the

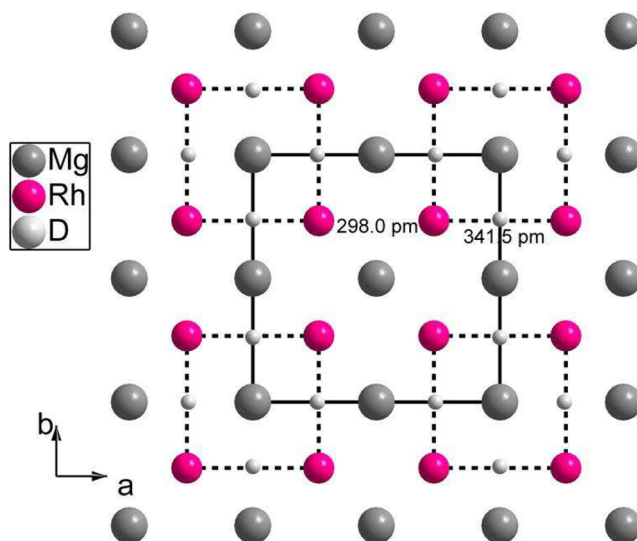


Figure 2. Crystal structure of MgRhH_{1-x} ($x = 0.06$) in a projection along the crystallographic c direction. The crystal structure was determined from the deuteride data.¹² Magnesium atoms are located at $z = 0$, rhodium and hydrogen atoms at $z = 1/2$. The dashed lines show tetrameric $[\text{Rh}_4\text{H}_4]$ units. The nearest Rh–Rh distances are also shown.

alkaline and alkaline earth metals. Of those, only the existence of Na_3RhH_6 has been verified. The hypothetical compounds Na_3RhH_4 and CaRhH are included for two reasons. First, the results provide information on the question of whether these compounds can be good candidates for synthetic approaches, although ultimately also other effects (beyond the scope of the present work) like entropy and phonon spectra will be relevant for estimating their thermodynamic stability. Second, the influence of the exchange by larger cations on the rhodium–rhodium interactions can improve the understanding of the chemical bonding in these interesting compounds.

II. COMPUTATIONAL APPROACH

We have studied theoretically the experimentally well-known complex lithium rhodium hydrides Li_3RhH_4 and Li_3RhH_6 as well as their sodium homologues, Na_3RhH_4 and Na_3RhH_6 , of which Na_3RhH_4 has not yet been characterized experimentally. Furthermore, we also studied the alkaline earth compound MgRhH_{1-x} . To avoid the theoretical treatment of partial occupancies, we have assumed full hydrogen occupancy ($x = 0$), which is close to the compound $\text{MgRhH}_{0.94}$ ($x = 0.06$) synthesized at high hydrogen gas pressure.

First, we performed structural relaxations of all compounds starting from the experimentally determined structural data of the deuterides. For the experimentally unknown Na_3RhH_4 , lattice constants and atomic positions of the homologue Li_3RhH_4 were used as initial guess. After complete structure optimization, (partial) densities of states (using an energy broadening of 0.1 eV), Crystal Orbital Hamilton Populations (COHPs),¹⁸ and Bader charges¹⁹ were calculated. The structural relaxation and the calculation of Bader charges were performed using the Vienna ab initio simulation package (VASP) together with the Projector Augmented Wave method.²⁰ An energy cutoff of 600 eV for the plane-wave expansion of the electronic orbitals was applied. When available, we used the experimentally determined structures as input structures and optimized lattice coordinates and internal coordinates. Symmetrically equivalent atoms were treated as being different. Moreover, for the SCF iterations we used a tolerance of 10^{-5} eV, and the structure was considered converged when the total energy changed less than 10^{-4} eV. For the Bader charge analysis, a very fine FFT grid was used. Exchange–correlation effects were treated with the generalized-gradient approximation of Perdew and Wang.²¹

Table 1. Space Groups as well as Experimental and Theoretical Lattice Constants for the Different Complex Hydrides of Our Study^a

material	space group	<i>a</i> (Å, exp.)	<i>a</i> (Å, calc.)	<i>b</i> (Å, exp.)	<i>b</i> (Å, calc.)	<i>c</i> (Å, exp.)	<i>c</i> (Å, calc.)
Li ₃ RhH ₄	<i>Cmcm</i>	3.883(1)	3.865	9.022(2)	8.968	8.891(2)	8.834
Li ₃ RhH ₆	<i>Pnma</i>	8.523(2)	8.512	4.797(1)	4.790	8.502(3)	8.495
Na ₃ RhH ₄	<i>Cmcm</i>	*	4.489	*	9.838	*	9.806
Na ₃ RhH ₆	<i>Pnma</i>	9.378(1)	9.378	5.285(1)	5.285	9.598(2)	9.598
MgRhH _{1-x}	<i>PA/mmm</i>	6.395(1)**	6.4192	=a**	=a	3.2368(7)**	3.28166

^aThe experimental parameters for Li₃RhH₄ are taken from ref 17, those for Li₃RhH₆ are from ref 7, and those for Na₃RhH₆ are from ref 6, respectively. Na₃RhH₄ is not known experimentally, and for MgRhH_{1-x} only data for the deuteride are available; see ref 11. "*" marks unknown data; "**" marks deuteride data.

Table 2. Atomic Positions for M₃RhH₆ from the Present Calculations in Comparison with Experimental Values^a

material	atom	position	coordinates (calc.)	coordinates (exp.)
Li ₃ RhH ₆	Li1	4c	(<i>x</i> , <i>z</i>) = (0.0458, 0.6258)	(<i>x</i> , <i>z</i>) = (0.057, 0.591)
	Li2	4c	(<i>x</i> , <i>z</i>) = (0.3978, 0.5190)	(<i>x</i> , <i>z</i>) = (0.368, 0.533)
	Li3	4c	(<i>x</i> , <i>z</i>) = (0.2170, 0.2447)	(<i>x</i> , <i>z</i>) = (0.229, 0.262)
	Rh	4c	(<i>x</i> , <i>z</i>) = (0.2275, 0.8942)	(<i>x</i> , <i>z</i>) = (0.222, 0.888)
	H1	8d	(<i>x</i> , <i>y</i> , <i>z</i>) = (0.3459, 0.4977, 0.9645)	(<i>x</i> , <i>y</i> , <i>z</i>) = (0.335, 0.490, 0.950)
	H2	8d	(<i>x</i> , <i>y</i> , <i>z</i>) = (0.1100, 0.4926, 0.8190)	(<i>x</i> , <i>y</i> , <i>z</i>) = (0.117, 0.503, 0.810)
	H3	4c	(<i>x</i> , <i>z</i>) = (0.1130, 0.0537)	(<i>x</i> , <i>z</i>) = (0.133, 0.057)
	H4	4c	(<i>x</i> , <i>z</i>) = (0.3348, 0.7352)	(<i>x</i> , <i>z</i>) = (0.339, 0.747)
Na ₃ RhH ₆	Na1	4c	(<i>x</i> , <i>z</i>) = (0.0521, 0.6248)	(<i>x</i> , <i>z</i>) = (0.047, 0.630)
	Na2	4c	(<i>x</i> , <i>z</i>) = (0.3968, 0.5349)	(<i>x</i> , <i>z</i>) = (0.408, 0.534)
	Na3	4c	(<i>x</i> , <i>z</i>) = (0.2055, 0.2558)	(<i>x</i> , <i>z</i>) = (0.217, 0.263)
	Rh	4c	(<i>x</i> , <i>z</i>) = (0.2274, 0.9022)	(<i>x</i> , <i>z</i>) = (0.218, 0.904)
	H1	8d	(<i>x</i> , <i>y</i> , <i>z</i>) = (0.3344, 0.4764, 0.9681)	(<i>x</i> , <i>y</i> , <i>z</i>) = (0.331, 0.475, 0.968)
	H2	8d	(<i>x</i> , <i>y</i> , <i>z</i>) = (0.1168, 0.4692, 0.8373)	(<i>x</i> , <i>y</i> , <i>z</i>) = (0.106, 0.469, 0.836)
	H3	4c	(<i>x</i> , <i>z</i>) = (0.1264, 0.0455)	(<i>x</i> , <i>z</i>) = (0.122, 0.044)
	H4	4c	(<i>x</i> , <i>z</i>) = (0.3209, 0.7550)	(<i>x</i> , <i>z</i>) = (0.307, 0.751)

^aM = Li or Na. The experimental results are taken from ref 7 for M = Li and from ref 6 for M = Na, respectively. The four equivalent 4c positions are given as (*x*, 1/4, *z*), (1/2 - *x*, 3/4, *z* - 1/2), (1 - *x*, 3/4, 1 - *z*), and (1/2 + *x*, 1/4, 1/2 - *z*). The eight equivalent 8d positions are given as (*x*, *y*, *z*), (1/2 - *x*, 1 - *y*, *z* - 1/2), (1 - *x*, 1/2 + *y*, 1 - *z*), (1/2 + *x*, 1/2 - *y*, 1/2 - *z*), (1 - *x*, 1 - *y*, 1 - *z*), (1/2 + *x*, *y*, 1/2 - *z*), (*x*, 1/2 - *y*, *z*), and (1/2 - *x*, 1/2 + *y*, *z* - 1/2).

Because the VASP program package applies plane waves as basis functions, it is nontrivial to obtain atom-resolved properties. We have, therefore, chosen to calculate COHPs and densities of state for the relaxed structures using the Spanish Initiative for Electronic Simulations with Thousands of Atoms 3.1 (SIESTA) program²² with pseudopotentials from the ABINIT database.^{23,24} In this case, exchange and correlation effects were treated with the generalized-gradient approximation of Perdew, Burke, and Enzerhof.²⁵ An energy cutoff of 150 Ry was applied in these calculations. For all calculations, *k*-space samplings were performed using a 16×16×8 (Li₃RhH₄, Li₃RhH₆, Na₃RhH₄, and Na₃RhH₆) or a 4×4×16 (MgRhH_{1-x} with a 2×2×1 supercell) Monkhorst–Pack grid, respectively. We checked that the results did not change when changing the *k*-space sampling or the energy cutoff.

III. RESULTS AND DISCUSSION

A. General Considerations on Rhodium–Rhodium Distances and Bonding. To give some benchmark values on the interatomic distances in compounds with and without rhodium–rhodium interactions, we shall first discuss those of lithium and magnesium rhodium hydrides.

Short rhodium–rhodium bonds are known to occur in a number of molecular inorganic compounds. For example, single rhodium–rhodium bonds are found in Rh²⁺ units coordinated by carboxylato, thiocarboxylato, or phosphine ligands in molecular compounds.²⁶ Typically, rhodium–rhodium distances vary between 235 and 245 pm in such complexes and are much shorter than the shortest ones observed in Li₃RhH₄

(387 pm) and MgRhH_{1-x} (298 pm, cf., Figures 1 and 2). Also, some dinuclear rhodium(I) complexes show short rhodium–rhodium distances albeit the absence of bonding between the metal atoms, for example, with arsanil- and phosphanylarylthiolato ligands, respectively.²⁷ The quasi-one-dimensional oxide Ba₉Rh₈O₂₄ contains an infinite Rh(IV) atom chain with 245 pm spacing.²⁸ A rhodium–rhodium distance of 274 pm is found in YbRhB₄ and related compounds.²⁹ However, while Rh–B and B–B bonding coexist in two-dimensional planar boron polyanions, which are connected by rhodium atoms, no binding rhodium–rhodium interaction was found. These examples illustrate the difficulty in predicting the nature of chemical bonding by restricting the discussion exclusively to interatomic distances.

In view of the different chemical nature of these compounds, however, it might be more suitable to compare the hydrides studied in this work with intermetallic compounds and other metal hydrides. Rhodium crystallizes in a cubic closest packing of atoms (copper-type structure) with a rhodium–rhodium distance of 270 pm.³⁰ In many rhodium-rich intermetallics and interstitial metal hydrides, short rhodium–rhodium distances occur as well, including 241 pm in La₂Rh₂Cd,³¹ 285 pm in CeRh₃,¹⁵ 288 pm in CeRh₃D_{0.84},¹⁵ and 317 pm in Mg₂RhD_{1.1}.¹³ Rhodium–rhodium distances in typical complex hydrides tend to be much larger and are usually well above 400 pm. Rare examples of shorter Rh–Rh distances are 364 pm in Ca₈Rh₆D₂₄,³² 364 pm in Ca₈Rh₅D₂₃,³² and 381 pm in

$\text{Sr}_8\text{Rh}_5\text{D}_{23}$.³³ The reported rhodium–rhodium distances of 387 pm in Li_3RhD_4 (Figure 1) and 298 pm MgRhD_{1-x} (Figure 2) together with the observed metal–deuterium coordination classifies the former compound to belong to the group of complex transition metal hydrides, while the latter is an interstitial hydride. However, because of the large spread of rhodium–rhodium distances within each group (vide supra), no clear assignment of metal–metal interactions can be made on the basis of geometric arguments alone. In the following, results from our theoretical calculations are used to quantitatively study the metal–metal interactions.

B. Li_3RhH_6 and Na_3RhH_6 . The shortest rhodium–rhodium distances are 487 pm in Li_3RhH_6 and 529 pm in Na_3RhH_6 . Such large distances between rhodium atoms make noteworthy covalent interactions between them very unlikely. The shortest rhodium–hydrogen distance of 165 and 167 pm, respectively, within the RhH_6 octahedra is typical for covalent bonding in anionic 18-electron hydridorhodate complexes in the solid state and can be rationalized by the sum of the covalent radii.³⁴ Therefore, these compounds may be expected to conform with a limiting ionic formula $(\text{M}^+)_3[\text{RhH}_6]^{3-}$ and be dominated by covalent rhodium–hydrogen bonding as well as ionic interactions between the alkaline cations and the complex anions. Furthermore, semiconducting behavior and the absence of metal–metal interactions are expected.

The calculated crystal structure parameters after relaxation show good agreement with the experimental data (see Tables 1 and 2). The calculated band gaps are 2.25 eV for the lithium compound (see Figure 3) and 2.85 eV for the sodium

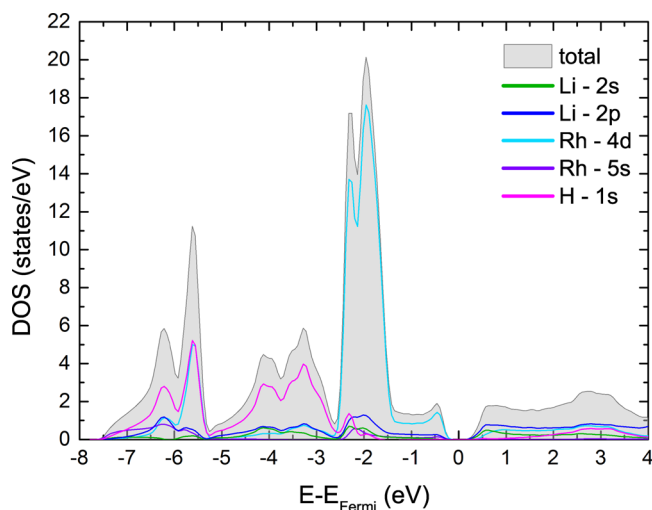


Figure 3. Partial and total density of states for Li_3RhH_6 .

compound, respectively. Because density-functional calculations like the ones of the present study tend to underestimate this gap, our results suggest that the materials are large-gap semiconductors. The results are consistent with the reported gray and colorless appearances.^{7,17} The most narrow bands in the density of states are due to Rh 4d and H 1s orbitals, which is a typical feature for complex 4d transition-metal hydrides (see Figure 3).

For Li_3RhH_6 and Na_3RhH_6 , the integrated Rh–Rh COHP over all occupied orbitals is close to zero (0.39 meV for the nearest-neighbor and 0.06 meV for the next-nearest-neighbor interactions for Li_3RhH_6 , shown in Figure 4, and -6.8 and -5.5 meV for the corresponding interactions for Na_3RhH_6),

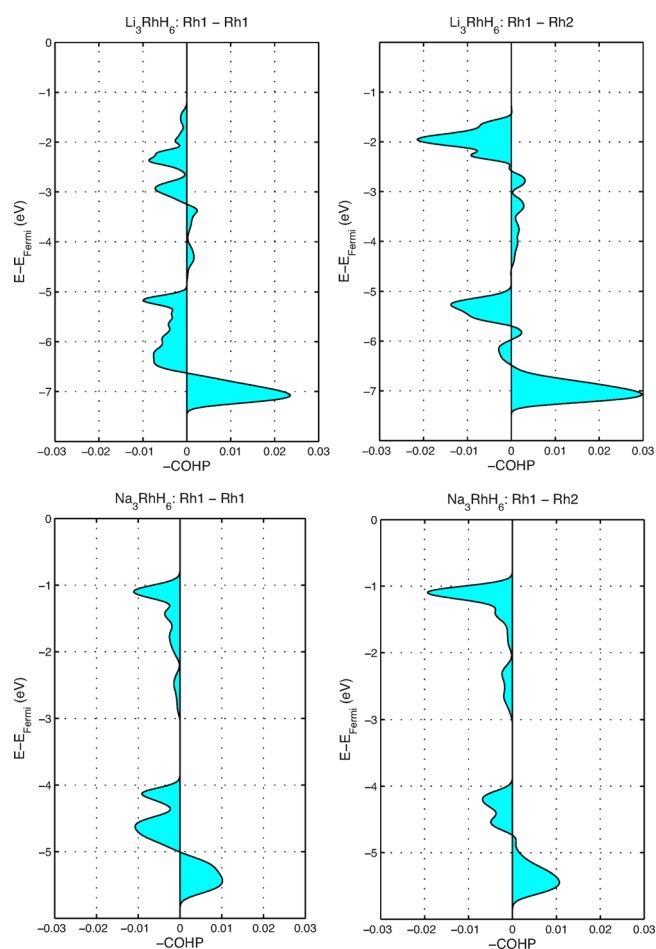


Figure 4. Crystal Orbital Hamilton Populations for (left) Rh–Rh nearest-neighbor and (right) Rh–Rh next-nearest-neighbor interactions for (upper part) Li_3RhH_6 and (lower part) Na_3RhH_6 . Notice the differences in the COHP scaling.

indicating the absence of metal–metal interactions. This can be explained by the effective shielding of the hydrogen atoms in the octahedral environment and the large rhodium–rhodium distances. Our calculations give accordingly the expected picture of chemical bonding in Li_3RhH_6 and Na_3RhH_6 with 18-electron complexes $[\text{RhH}_6]^{3-}$ and no significant metal–metal bonding. This also suggests that our theoretical approach is well suited for such ternary rhodium hydride compounds, which is in agreement with results of other, similar studies (see, for example, refs 35,36).

C. Li_3RhH_4 and Na_3RhH_4 . While the calculated lattice parameters and most of the internal structural parameters for Li_3RhH_4 agree reasonably well with experimental data, we observe a larger discrepancy for the Li1 positions (see Table 3) as compared to all other investigated compounds. In this regard, it is, however, important to notice the very good agreement for the rhodium atoms, which are in the focus of the present study. Hence, we consider the main results of our calculations to be affected very little by the discrepancies between experimental and calculated lithium and hydrogen position.

For Li_3RhH_4 , the COHPs for Rh atoms involved in two $[\text{RhH}_4]$ units lying on top of each other along the crystallographic a axis (Figure 1) are depicted in Figure 5. Both bonding and antibonding interactions can be identified,

Table 3. Atomic Positions for M_3RhH_4 from the Present Calculations in Comparison with Experimental Values^a

material	atom	position	coordinates (calc.)	coordinates (exp.)
Li_3RhH_4	Li1	8f	(y, z) = (0.8396, 0.0729)	(y, z) = (0.764, 0.074)
	Li2	4c	y = 0.5167	y = 0.562
	Rh	4c	y = 0.2070	y = 0.203
	H1	8f	(y, z) = (0.0683, 0.3776)	(y, z) = (0.055, 0.381)
	H2	8f	(y, z) = (0.3363, 0.1121)	(y, z) = (0.355, 0.125)
	Na_3RhH_4	Na1	8f	(y, z) = (0.8371, 0.0771)
Na2		4c	y = 0.5212	
Rh		4c	y = 0.2037	
H1		8f	(y, z) = (0.0767, 0.3654)	
H2		8f	(y, z) = (0.3216, 0.1243)	

^aM = Li or Na. The experimental results are taken from ref 17 for M = Li, whereas there are no experimental values for M = Na, respectively. The four equivalent 4c positions are given as (0, y, 1/4), (0, 1 - y, 3/4), (1/2, y - 1/2, 1/4), and (1/2, 1/2 - y, 3/4). The eight equivalent 8d positions are given as (x, y, z), (0, 1 - y, 1/2 + z), (0, y, 1/2 - z), (0, 1 - y, 1 - z), (1/2, y - 1/2, z), (1/2, 3/2 - y, 1/2 + z), (1/2, y - 1/2, 1/2 - z), and (1/2, 1/2 - y, 1 - z).

although the total interaction is rather weak: the integral of the COHP over all occupied bands is just 0.031 eV. For comparison, the integral of the COHP for the Rh–H interactions equals 0.854 eV. This indicates that the dashed lines in Figure 1 indeed correspond to partly covalent bonds, albeit not very strong. By comparing with the partial DOS (see Figure 6), both bonding and antibonding interactions can be assigned to the Rh 4d orbitals. However, interactions between next-nearest Rh neighbors can be ignored.

The calculated band gap is 0.3 eV, that is, considerably smaller than in Li_3RhH_6 and Na_3RhH_6 . The bands from the Rh 4d and the H 1s orbitals are again the most narrow (which is typical for complex hydrides), although to a lesser extent than in Li_3RhH_6 and Na_3RhH_6 . This suggests that the description with a limiting ionic formula as above for Li_3RhH_6 and Na_3RhH_6 is less appropriate for Li_3RhH_4 . The small band gap is consistent with the metallic luster of the compound observed experimentally¹⁷ and the metal–metal interactions along the $[\text{RhH}_4]$ stacks (Figure 1).

For the hypothetical homologue Na_3RhH_4 , the Rh–Rh COHP results show the same finding (see Figure 5) even though the bonding interactions are about one-third weaker than for the lighter homologue. Bands formed by Rh 4d and H 1s orbitals are narrower than those for the lithium compound. Because of this stronger localization, the calculated band gap of 0.44 eV is slightly larger. This might be traced back to the reduced rhodium–rhodium interactions, mainly due to the longer Rh–Rh distances of 449 pm (at this place it is worth emphasizing that calculations like those of the present study may predict values for the gap that are significantly underestimated, making it very difficult to make accurate statements about this property, whereas the bonding properties of the systems are well described). A limiting ionic formula according to $(M^+)_3[\text{RhH}_4]^{3-}$ with 16-electron complex anions is thus more appropriate for the sodium than for the lithium compound. Interestingly, the Rh–H distance is almost the

same in M_3RhH_4 (M = Li, Na), indicating that the cationic matrix has little effect on the RhH_4 building units.

D. $MgRhH_{1-x}$ and $CaRhH_{1-x}$. For the compound $MgRhH_{1-x}$ with varying hydrogen content, the formula $MgRhH$ was used, assuming that the chemical behavior does not differ from that of the known compound $MgRhH_{0.94}$. We then find a reasonable agreement between experimental and calculated crystal structure parameters. The slightly larger lattice parameters can be explained through the differences in hydrogen content between the experimentally and the theoretically studied systems. The COHPs are depicted in Figure 7. Here, the next-nearest Rh neighbor (Rh2–Rh2) COHPs characterize the interactions among the rhodium atoms within a $[\text{Rh}_4\text{H}_4]$ unit, and Rh–H COHPs characterize those of Rh and H within such units. On the other hand, the nearest Rh neighbor (Rh1–Rh2) COHPs describe the interactions between the units. The Rh–Rh interactions within the $[\text{Rh}_4\text{H}_4]$ units show a strong antibonding character, whereas the Rh2–H interactions are strongly binding. Between the rhodium atoms of different $[\text{Rh}_4\text{H}_4]$ units, a weaker binding interaction can be identified. The integral (0.061 eV) is actually larger than what we found for the binding interactions in Li_3RhH_4 , a fact that is in good agreement with the short Rh–Rh distances of only 295.35 pm. Even the distance between the rhodium atoms within one unit is slightly smaller than expected for such an antibonding character. The latter might be due to the presence of the hydrogen atom in the middle of the sides of the squares.

The compound is a metal with localized Rh 4d states just below the Fermi level. The metallic character can be mainly attributed to the Mg 3p and the Rh 4d states and is in good agreement with the metallic appearance of the samples.^{12,13} The orbitals of the bands formed from the Rh 4d and H 1s functions are less localized as compared to Li_3RhH_4 , which indicates an even stronger deviation from a typical complex hydride.

To estimate the charges of the $[\text{Rh}_4\text{H}_4]$ units, a charge analysis according to Bader was carried out. The resulting Bader populations are listed in Table 4. According to those, rhodium is negatively charged, resulting in a formal d^{10} -system. The charge of magnesium is approximately 1.5 and therefore smaller than the formal charge of +2. Similarly, the charge of the hydride, –0.4, is less negative than expected. Using the Bader charge and neglecting a possible charge delocalization within the $[\text{Rh}_4\text{H}_4]$ units, such a unit carries a formal charge of $4 \cdot Q_{\text{Rh}} + 4 \cdot Q_{\text{H}} = 4 \cdot (-1.14) + (-0.4) \approx -6$. Also, the calculated Bader volumes of the individual atoms (see Table 4) correspond well with their available space in the crystal (see Figure 8). For the sake of comparison, we give in Table 4 also the Mulliken gross populations. These give values significantly different from those of the Bader analysis, but it is well-known that Mulliken populations are useful when studying changes but not in providing absolute values for atomic charges. For the latter, the Bader charges are much more reliable.

The competition between bonding and antibonding interactions forces the rhodium atoms into a 4^4 net. Hydrogen, on the other hand, by being placed between antibonding rhodium atoms acts like a “glue” and forms a 4.8^2 net, that is, a tiling of squares and octagons. The hydrogen atoms are slightly displaced, resulting in a 3° deviation from a straight connection line between the rhodium atoms (see Figure 8). This might be due to a repulsion between the negatively charged hydridic atoms. Furthermore, the differences in the magnesium–

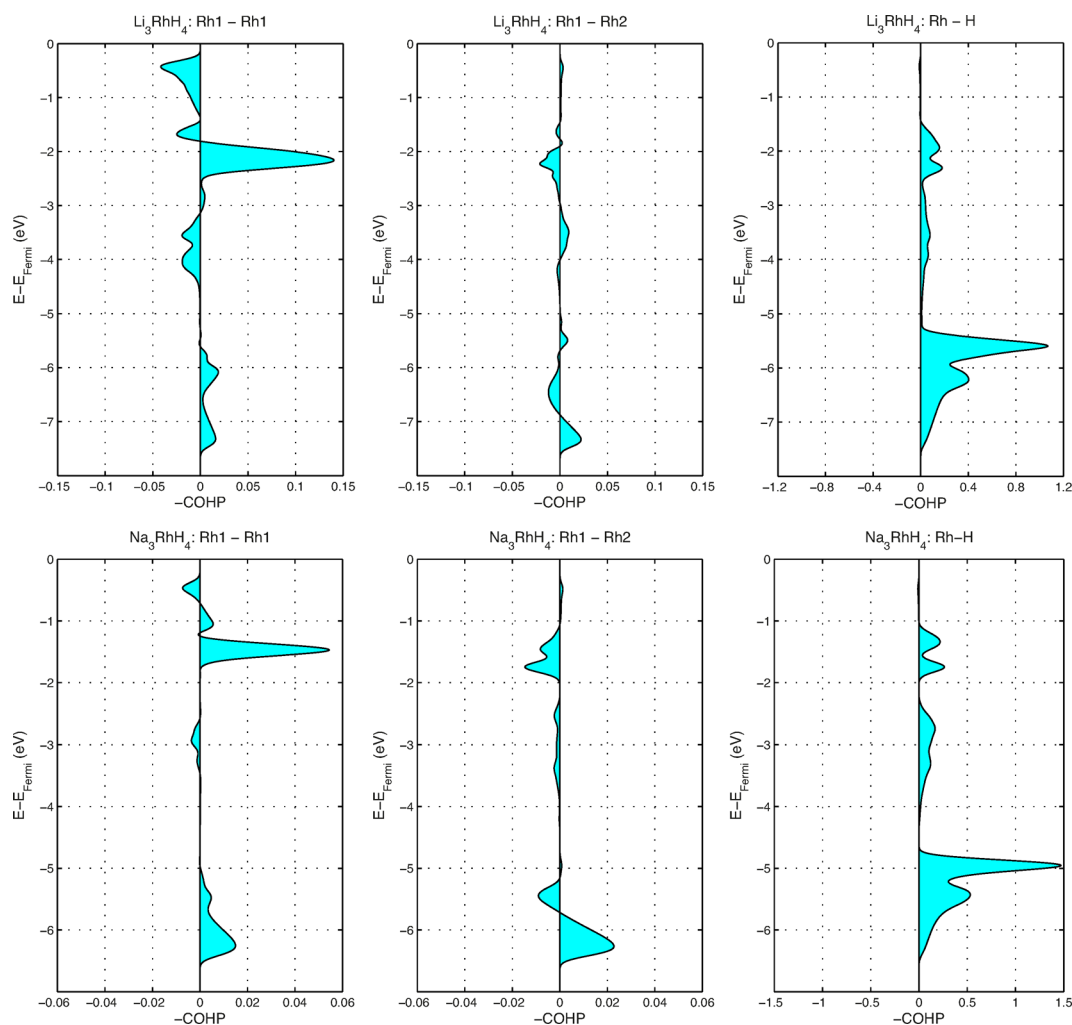


Figure 5. Crystal Orbital Hamilton Populations for (left) Rh–Rh nearest-neighbor and (right) Rh–Rh next-nearest-neighbor interactions for (upper part) Li_3RhH_4 and (lower part) Na_3RhH_4 . Notice the differences in the COHP scaling.

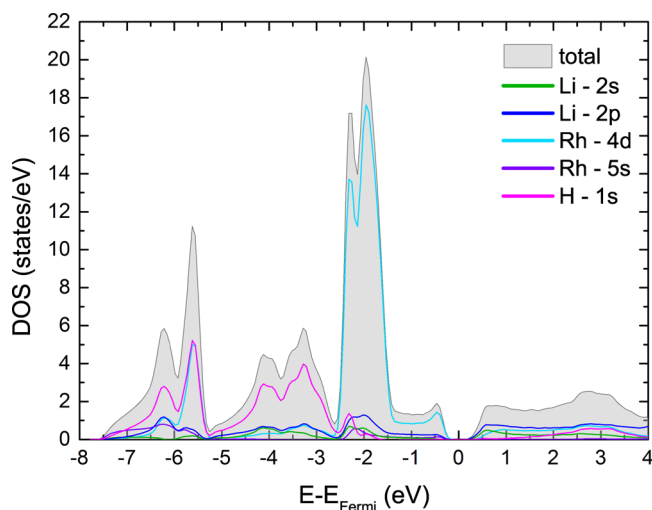


Figure 6. Partial and total density of states for Li_3RhH_4 .

hydrogen distances (experimental Mg–D distances of 223 pm for the 4-fold coordinated and 233 pm for the 8-fold coordinated Mg atom) are reduced by this off-line position. The dashed lines outlining the tetrameric $[\text{Rh}_4\text{H}_4]$ units in Figure 2 do not seem to describe the bonding situation well.

More appropriate is to describe the crystal structure as consisting of RhH_2 units with strong Rh–H bonding as primary building blocks. Four of those are joined together by rhodium–rhodium bonding to form Rh_4 squares (see dashed lines in Figure 8). Linking these units by common hydrogen atoms results in an infinite two-dimensional layer ${}^2_\infty[(\text{RhH}_{2/2})_4]$. These extended Rh–H polyanions alternate with magnesium layers along the crystallographic c axis as shown in the lower part in Figure 8.

The importance of the bonding Rh–Rh interactions for the stability of the compound is further illustrated by the results of our attempt to calculate structural and electronic properties of the hypothetical, higher homologue CaRhH . Assuming the same structural model as for MgRhH , no convergence for the structural relaxation could be achieved. This may point to a lack of stability for this hypothetical compound.

E. Chemical Bonding in Ternary Rhodium and Ternary Ruthenium Hydrides. We now return to the initially posed questions concerning the binding situation of ternary rhodium hydrides. The answer to the question of whether significant rhodium–rhodium interactions exist in Li_3RhH_4 and MgRhH is clearly “yes”. They are one-dimensional in Li_3RhH_4 and two-dimensional and about 3 times stronger in case of MgRhH . As for metallic properties, Li_3RhH_4 seems to be a small-band gap semiconductor, whereas the stronger metal–metal interaction

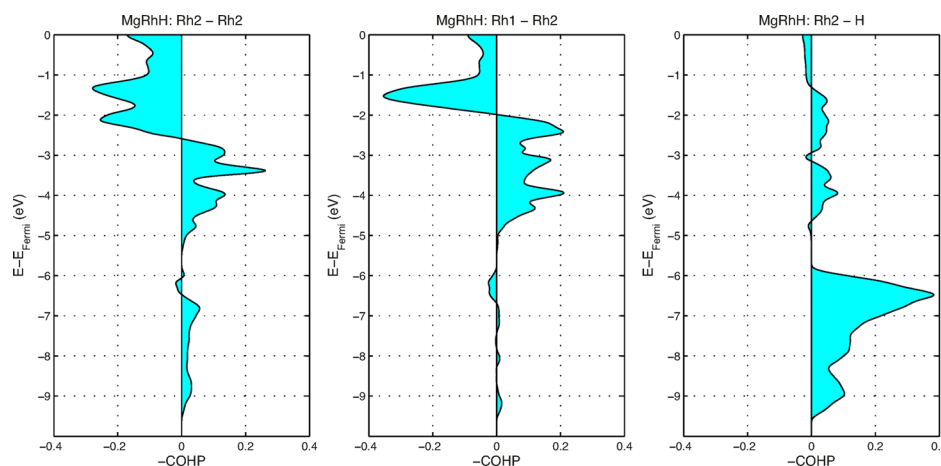


Figure 7. Crystal Orbital Hamilton Populations for (from left to right) Rh–Rh next-nearest-neighbor, Rh–Rh nearest-neighbor, and Rh–H interactions for MgRhH_{1-x} with $x = 0$.

Table 4. Atomic Valence Populations and Volumes for MgRhH_{1-x} ^a

atom	Wyckoff position	Bader population	Bader volume (\AA^3)	N_i
Mg	1a	0.4186	6.0153	1.8
Mg	1c	0.8934	5.3370	1.8
Mg	2f	0.4550	5.7065	1.8
Rh	4k	10.1405	22.9985	9.155
H	4m	1.4023	5.1163	1.035

^aThe Bader populations give the number of valence electrons within the atomic volumes according to the Bader analysis, whereas N_i gives the Mulliken gross populations. For the neutral atoms, the numbers would equal 2, 9, and 1 for Mg, Rh, and H, respectively.

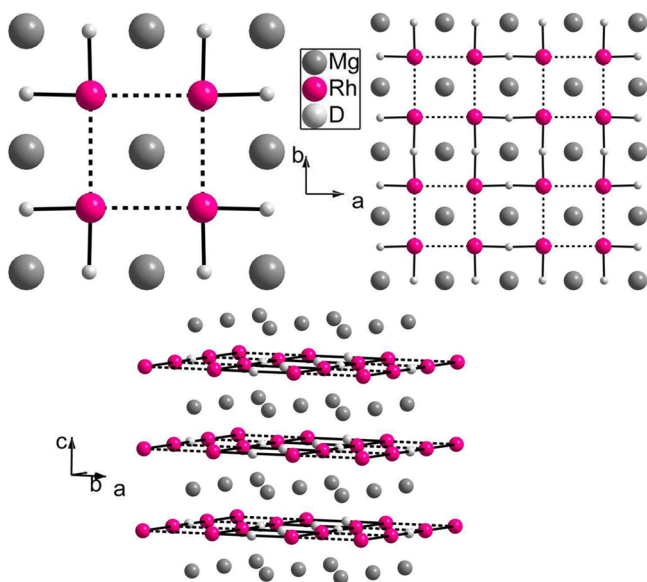


Figure 8. Calculated crystal structure of MgRhH in (upper part) a projection along crystallographic c with magnesium atoms (large, gray) at the height $z = 0$, rhodium (medium size, red) and hydrogen atoms (small, white) at $z = 1/2$. Solid lines represent Rh–H bonds; dashed lines represent Rh–Rh bonds. Note the slight off-line position of hydrogen. Unit cell edges are omitted for clarity. Left, one unit cell showing $(\text{RhH}_2)_4$ as building block; right, four unit cells showing the linkage to ${}^\infty[(\text{RhH}_{2/2})_4]$ layers. The lower part presents a view almost perpendicular to the crystallographic c axis showing the stacking of Mg and $[\text{RhH}_{2/2}]_4$ layers.

and the increased dimensionality result in metallic properties for MgRhH . The tetrameric $[\text{Rh}_4\text{H}_4]$ units do indeed have importance in the description of chemical bonding in MgRhH . However, the situation is made somewhat more complicated by the antibonding Rh–Rh interactions within these units and the bonding between rhodium atoms of adjacent units, thus forming Rh_4 squares. The influence of lithium and magnesium is not negligible. Calculations for the analogous sodium compound Na_3RhH_4 show considerably reduced metal–metal interactions leading to a destabilization of the compound, and for the hypothetical CaRhH it was not even possible to theoretically determine a stable structure. The main reason for this failure is most likely related to the atom size. For the larger sodium and calcium matrices, rhodium–rhodium distances are stretched beyond the limit of significant interaction, which in case of CaRhH leads to a complete destabilization of the structure.

In case of the lithium and sodium rhodium hydrides, the analysis of Mulliken gross populations of the valence electrons may give additional insight (see Table 5). When comparing the charges assigned to the rhodium atoms, those in the sodium compounds are larger than those in the lithium compounds. This can be attributed to a more complete charge transfer from the less electronegative sodium to the hydridometalate anions and is in agreement with the earlier finding that sodium compounds comply better with the picture of the classical complex transition-metal hydrides than the lithium compounds. For Li_3RhH_4 , the Mulliken populations correspond to a formal oxidation number of Rh(I). The observed planar RhH_4 coordination is typical for the according d^8 configuration and also found in other hydrides with d^8 transition metals such as in Na_2PdH_4 ,³⁷ K_2PdH_4 ,³⁸ and Na_2PtH_4 .¹ Rhodium atoms in M_3RhH_4 compounds carry a larger number of valence electrons than in the corresponding M_3RhH_6 compounds ($M = \text{Li}, \text{Na}$) (see Table 5), which may simply be attributed to the number of hydrogen atoms in the coordination sphere (four vs six) because hydrogen is the most electronegative element in the system $M\text{–Rh–H}$. This feature may also be expected in view of the formal rhodium oxidation numbers of +I in the former and +III in the latter compounds. The H3 atom in M_3RhH_6 with the smallest charge has the longest distance to neighboring M atoms ($M = \text{Li}, \text{Na}$). Li2 in Li_3RhH_4 carries a larger positive charge (see Table 5) than Li1, because of a higher coordination with hydrogen. The good correspondence of these results with

Table 5. Mulliken Gross Populations, N_i , for the Valence Electrons of the Compounds of the Present Study^a

element	material	label	position	N_i	element	material	label	position	N_i
Li	Li ₃ RhH ₄	Li1	8f	0.882	Na	Na ₃ RhH ₄	Na1	8f	0.630
		Li2	4c	0.640			Na2	4c	0.631
	Li ₃ RhH ₆	Li1	4c	0.472		Na ₃ RhH ₆	Na1	4c	0.492
		Li2	4c	0.614			Na2	4c	0.486
		Li3	4c	0.511			Na3	4c	0.512
Rh	Li ₃ RhH ₄	Rh1	4c	8.830	Rh	Na ₃ RhH ₄	Rh1	4c	9.212
	Li ₃ RhH ₆	Rh1	4c	8.608	Na ₃ RhH ₆	Rh1	4c	9.020	
H	Li ₃ RhH ₄	H1	8f	1.207	H	Na ₃ RhH ₄	H1	8f	1.235
		H2	8f	1.177			H2	8f	1.213
	Li ₃ RhH ₆	H1	8d	1.333	Na ₃ RhH ₆	H1	8d	1.264	
		H2	8d	1.268		H2	8d	1.235	
		H3	4c	1.210		H3	4c	1.222	
		H4	4c	1.383		H4	4c	1.272	

^aThe positions and labels refer to Tables 2 and 3. For the neutral atoms, the Mulliken populations would equal 1, 1, 9, and 1 for Li, Na, Rh, and H, respectively.

crystal-chemical considerations underlines the reliability of the calculated data.

Metal–metal interactions like those found here in Li₃RhH₄ and MgRhH are rare but not unique to rhodium in metal hydrides. They are also found in some magnesium ruthenium hydrides. While Mg₂RuH₆ and Mg₃RuH₆ are classical complex hydrides with 18-electron complexes [RuH₆]⁴⁻ and [RuH₅]⁵⁻, respectively,^{39,40} in the hydrogen-poorer compounds Mg₂RuH₄ and Mg₃RuH₃, however, such a simple picture of the chemical bonding situation may not be appropriate. The hydrogen atoms in diamagnetic Mg₂RuH₄ surround ruthenium in a saddle-like arrangement with the closest Ru–Ru distance being 324 pm within infinite [RuH₄] chains.⁴¹ In those chains, the Ru atoms are arranged in a zigzag pattern. The anion can be described as either a 16-electron complex [RuH₄]⁴⁻ or a polymer with infinite [RuH₄] zigzag chains and Ru–Ru bonding. A similar situation occurs in Mg₃RuH₃ for which dinuclear [Ru₂H₆]¹²⁻ units with Ru–Ru bonding were proposed instead of 17-electron mononuclear complexes.⁴² The significance of ruthenium–ruthenium bonding in these compounds, however, is still controversially discussed.^{4,5}

IV. CONCLUSIONS

We have studied the chemical bonding and electronic properties of the complex rhodium hydrides Li₃RhH₄, Li₃RhH₆, Na₃RhH₄, Na₃RhH₆, and MgRhH with special focus on the existence of covalent Rh–Rh interactions. For Li₃RhH₄ and the hypothetical Na₃RhH₄ whose structures feature planar [RhH₄]³⁻ units, such interactions could be identified along $\frac{1}{\infty}$ [RhH₄] stacks, with the interaction in the lithium compound being much stronger than that in the sodium compound. Both compounds are small-band gap semiconductors. For the hydrides Li₃RhH₆ and Na₃RhH₆ featuring isolated octahedral [RhH₆]³⁻ units, no metal–metal interaction could be detected, and thus a description with a limiting ionic formula (M⁺)₃[RhH₆]³⁻ (M = Li, Na) for these semiconducting compounds with relatively large band gaps seems appropriate. For the alkaline earth hydride MgRhH, strong Rh–Rh interactions were found. MgRhH certainly does not qualify for the description as a classical complex metal hydride and has metallic properties. Instead, its crystal structure features RhH₂ units with strong Rh–H bonding as primary building blocks, joined together by rhodium–rhodium bonding to form Rh₄ squares. Further connection is realized by sharing hydrogen

atoms to form infinite two-dimensional $\frac{2}{\infty}$ [(RhH_{2/2})₄] layers. For the hypothetical higher homologue CaRhH, the difficulties of the theoretical calculations may indicate a lack of stability. Li₃RhH₄ and MgRhH_{1-x} are thus interesting examples for metal–metal bonding in ternary metal hydrides. While such interactions are one-dimensional and weak in the lithium compound, they are considerably stronger and two-dimensional in MgRhH_{1-x}, resulting in metallic properties.

AUTHOR INFORMATION

Corresponding Authors

*Tel.: +49 (0)681 302 3856. E-mail: m.springborg@mx.uni-saarland.de.

*Tel.: +49 (0)341 97 36201. E-mail: holger.kohlmann@uni-leipzig.de.

Notes

The authors declare no competing financial interest.

REFERENCES

- (1) Bronger, W.; Müller, P.; Schmitz, D.; Spittank, H. *Z. Anorg. Allg. Chem.* **1984**, *516*, 35–41.
- (2) Didisheim, J.-J.; Zolliker, P.; Yvon, K.; Fischer, P.; Schefer, J.; Gubelmann, M.; Williams, A. F. *Inorg. Chem.* **1984**, *23*, 1953–1957.
- (3) Kohlmann, H.; Moyer, R. O., Jr.; Hansen, T.; Yvon, K. *J. Solid State Chem.* **2003**, *174*, 35–43.
- (4) Miller, G. J.; Deng, H.; Hoffmann, R. *Inorg. Chem.* **1994**, *33*, 1330–1339.
- (5) Orgaz, E.; Aburto, A. *J. Phys. Chem. C* **2008**, *112*, 15586–15594.
- (6) Bronger, W.; Müller, P.; Kowalczyk, J.; Auffermann, G. *J. Alloys Compd.* **1991**, *176*, 263–268.
- (7) Bronger, W.; Gehlen, M.; Auffermann, G. *Z. Anorg. Allg. Chem.* **1994**, *620*, 1983–1985.
- (8) Heckers, U.; Niewa, R.; Jacobs, H. *Z. Anorg. Allg. Chem.* **2001**, *627*, 14011404.
- (9) Weller, M. T.; Henry, P. F.; Ting, V. P.; Wilson, C. C. *Chem. Commun.* **2009**, 2973–2989.
- (10) Ting, V. P.; Henry, P. F.; Kohlmann, H.; Wilson, C. C.; Weller, M. T. *Phys. Chem. Chem. Phys.* **2010**, *12*, 2083–2088.
- (11) Bonhomme, F.; Yvon, K.; Fischer, P. *J. Alloys Compd.* **1992**, *186*, 209–215.
- (12) Bonhomme, F. Synthèse et caractérisation structurale d'hydrures ternaires contenant du magnésium et un métal de transition du groupe VIII. Thesis No. 2720, University of Geneva, 1995.
- (13) Bonhomme, F.; Selvam, P.; Yoshida, M.; Yvon, K.; Fischer, P. *J. Alloys Compd.* **1992**, *178*, 167–172.

- (14) Buschow, K. H. J.; Cohen, R. L.; West, K. W. *J. Appl. Phys.* **1977**, *48*, 5289–5295.
- (15) Kohlmann, H.; Müller, F.; Stöwe, K.; Zalga, A.; Beck, H. P. *Z. Anorg. Allg. Chem.* **2009**, *635*, 1407–1411.
- (16) Kohlmann, H. *Z. Kristallogr.* **2009**, *224*, 454–460.
- (17) Bronger, W.; Gehlen, M.; Auffermann, G. *J. Alloys Compd.* **1991**, *176*, 255–262.
- (18) Dronskowski, R.; Blöchl, P. E. *J. Phys. Chem.* **1993**, *97*, 86178624.
- (19) Bader, R. F. W. *Atoms in Molecules — a Quantum Theory*; Clarendon Press: Oxford, 1990.
- (20) Blöchl, P. E. *Phys. Rev. B* **1994**, *50*, 17953–17979.
- (21) Perdew, J. P.; Wang, Y. *Phys. Rev. B* **1992**, *45*, 13244–13249.
- (22) Soler, J. M.; Artacho, E.; Gale, J. D.; Garcia, A.; Junquera, J.; Ordejón, P.; Sánchez-Portal, D. *J. Phys.: Condens. Matter* **2002**, *14*, 2745.
- (23) Gonze, X.; Amadon, B.; Anglade, P.-M.; Beuken, J.-M.; Bottin, F.; Boulanger, P.; Bruneval, F.; Caliste, D.; Caracas, R.; Côté, M.; Deutsch, T.; Genovese, L.; Ghosez, Ph.; Giantomassi, M.; Goedecker, S.; Hamann, D. R.; Hermet, P.; Jollet, F.; Jomard, G.; Leroux, S.; Mancini, M.; Mazevet, S.; Oliveira, M. J. T.; Onida, G.; Pouillon, Y.; Rangel, T.; Rignanese, G.-M.; Sangalli, D.; Shaltaf, R.; Torrent, M.; Verstraete, M. J.; Zerah, G.; Zwanziger, J. W. *Comput. Phys. Commun.* **2009**, *180*, 2582–2615.
- (24) Gonze, X.; Rignanese, G.-M.; Verstraete, M.; Beuken, J.-M.; Pouillon, Y.; Caracas, R.; Jollet, F.; Torrent, M.; Zerah, G.; Mikami, M.; Ghosez, Ph.; Veithen, M.; Raty, J.-Y.; Olevano, V.; Bruneval, F.; Reining, L.; Godby, R.; Onida, G.; Hamann, D. R.; Allan, D. C. *Z. Kristallogr.* **2005**, *220*, 558–562.
- (25) Perdew, J. P.; Burke, K.; Ernzerhof, M. *Phys. Rev. Lett.* **1996**, *77*, 3865–3868.
- (26) Chifotides, H. T.; Dunbar, K. R. Rhodium Compounds. In *Multiple Bonds between Metal Atoms*, 3rd ed.; Cotton, F. A., Murillo, C. A., Walton, R. A., Eds.; Springer Verlag: Berlin, 2005; Chapter 12, pp 465–589.
- (27) Hildebrand, A.; Sárosi, M. B.; Lönnecke, P.; Silaghi, L.; Dumitrescu, Hey-Hawkins, E. *Rev. Roum. Chim.* **2010**, *55*, 885–896.
- (28) Boulahya, K.; Hernando, M.; Varela, A.; Gonzalez-Calbet, J. M.; Parras, M.; Amador, U.; Martinez, J. L. *Eur. J. Inorg. Chem.* **2002**, *2002*, 805–810.
- (29) Veremchuk, I.; Mori, T.; Prots, Yu.; Schnelle, W.; Leithe-Jasper, A.; Kohout, M.; Grin, Yu. *J. Solid State Chem.* **2008**, *181*, 19831991.
- (30) Hull, A. W. *Phys. Rev.* **1921**, *17*, 571–588.
- (31) Stadler, F.; Fickenscher, T.; Pöttgen, R. *Z. Naturforsch., B* **2001**, *56*, 1241–1244.
- (32) Bronger, W.; Breil, L. *Z. Anorg. Allg. Chem.* **1998**, *624*, 1819–1822.
- (33) Bronger, W.; Beißmann, R.; Ridder, G. *J. Alloys Compd.* **1994**, *203*, 91–96.
- (34) Yvon, K. Hydrides: Solid State Transition Metal Complexes. In *Encyclopedia of Inorganic Chemistry*; King, R. B., Ed.; Wiley: New York, 1994; Vol. 3, pp 1401–1420.
- (35) Burghaus, J.; Wessel, M.; Houbon, A.; Donskowsky, R. *Inorg. Chem.* **2010**, *49*, 10148–10155.
- (36) Yamada, T.; Deringer, V. L.; Dronskowski, R.; Yamane, H. *Inorg. Chem.* **2012**, *51*, 4810–4816.
- (37) Bronger, W.; Auffermann, G. *J. Alloys Compd.* **1995**, *228*, 119121.
- (38) Kadir, K.; Kritikos, M.; Noreus, D.; Andresen, A. F. *J. Less-Common Met.* **1991**, *172174*, 3641.
- (39) Huang, B.; Bonhomme, F.; Selvam, P.; Yvon, K.; Fischer, P. *J. Less-Common Met.* **1991**, *171*, 301–311.
- (40) Bronger, W.; Jansen, K.; Auffermann, G. *J. Alloys Compd.* **1993**, *199*, 47–51.
- (41) Bonhomme, F.; Yvon, K.; Triscone, G.; Jansen, K.; Auffermann, G.; Müller, P.; Bronger, W.; Fischer, P. *J. Alloys Compd.* **1992**, *178*, 161–166.
- (42) Bonhomme, F.; Yvon, K.; Fischer, P. *J. Alloys Compd.* **1992**, *186*, 309–314.